Ceratonia siliqua pulp extracts as a green corrosion inhibitor for mild carbon steel in 1 M HCl

M.A. Almomani, M.T. Hayajneh and W.M. AlSharman

Industrial Engineering Department, Faculty of Engineering, Jordan University of Science and Technology, P.O. Box 3030, Irbid, 22110, Jordan
**E-mail: maalmomani7@just.edu.jo*

Abstract

The anticorrosion behaviour of *Ceratonia silique L.* pulp extract on mild steel in 1 M HCl solution was studied by employing a potentiodynamic polarization test (PDP) and weight loss test with different concentrations at room temperature. The obtained results suggested that the *C. siliqua* pulp extract is an excellent corrosion inhibitor and its inhibition efficiency is both concentration and time-dependent. Inhibition efficiency η(%) is observed to increase with an increase in *C. siliqua* pulp extract concentration and an increase in immersion time. The maximum inhibition efficiency of 92.32% was observed at a concentration of 800 ppm at room temperature. As evident by PDP the *C. siliqua* pulp extract behaves as a mixed-type inhibitor, and the cathodic impact is predominant. The inhibitor adsorption on the mild steel surface is following the Langmuir adsorption isotherm, and the adsorption mechanism is physical adsorption. *C. siliqua* pulp extract is a suitable corrosion inhibitor for mild steel in 1 M HCl solution.

Keywords: *corrosion, green inhibitor, mild steel, polarization, Ceratonia silique L.*

Received: November 13, 2022. Published: June 25, 2023 doi: 10.17675/2305-6894-2023-12-2-23

1. Introduction

The outstanding mechanical properties of steel, and its relatively low cost make steel one of the most widely used alloys in the manufacturing and construction industries [1, 2]. Its applications range from very simple products to large and complex products, *i.e.*, chemical reactors, storage tanks, heat exchangers, transporting pipelines for gases and oils, and boilers systems [3]. The exposure of steel to high temperatures results in the formation of scales and oxides that have to be removed prior to further processing. This can be done by a special treatment known as pickling and using some chemical agents or acid solutions, *i.e.*, hydrochloric acid (HCl) [4]. The further exposure of the steel surface to these chemicals after scale removal speeds up its corrosion, causing material damage and significant economic losses. It was estimated that corrosion destroyed about 150 million tons of steel every year. Therefore, controlling steel corrosion is necessary to lessen these losses [5, 6].

The use of corrosion inhibitors is the easiest and most economical and most effective method for protecting metal against corrosion during acidic treatments because of their ease

of use as they can be applied without the need of changing the process and equipment, as they act quickly to protect against corrosion. These corrosion inhibitors are generally added in small quantities to acidic solutions to reduce metal dissolution and protect it from destruction [7, 8].

Due to their efficiency across a wide range of temperatures at relatively low concentrations and superior solubility, organic corrosion inhibitors have been widely employed in the industry [9]. Organic inhibitors are unfortunately harmful to human health and the environment, expensive, and poisonous [4]. The use of these harmful inhibitors has recently been outlawed by numerous international organizations. Additionally, the harmful properties of these inhibitors drove researchers to look for alternatives, which opened the door for the use of green corrosion inhibitors, which are often non-toxic, environmentally safe, and biodegradable natural product inhibitors [10]. These inhibitors, which have been employed for numerous metals including copper, aluminum, and mild steel, are often obtained from natural materials collected from the roots, leaves, bark, fruits, seeds, and medical plants [11]. In addition, chemical substances such as alkaloids, flavonoids, amino acids, heteroatoms, tannins, and nitrogen-based chemicals are abundant in green corrosion inhibitors [12]. These chemical compounds are widely distributed and contain a variety of aromatic rings, functional groups, aliphatic chains, heterocyclic rings, and functional moieties as well as polar and nonpolar compounds that contain nitrogen and oxygen. These substances can be adsorbed on the metal surface and effectively shield it from corrosion attacks [13].

The Jordanian environment contains many types of unique trees, including Carob (*Ceratonia Siliqua L.*), which is a member of the legume family (Fabaceae) [14]. Carob powder is obtained after removing the seeds from fruit pods [15]. By weight, the pulp (90%) and the seeds (10%) are the main components of the Carob pod [16]. The pods are mainly used in the food industry as an antioxidant due to their polyphenol-rich composition, they contain a high concentration of condensed tannins (16–20%), which are composed of flavan-3-ol groups, and their galloyl esters, garlic acid, (+)-catechin, (–)-epicatechingallate, quercetin glycosides, and (–)-epigallocatechingallate [17].

Recently, researchers examined the potential use of Carob extracts as a green organic corrosion inhibitor for carbon steel, copper, and brass. Abbout *et al.* [18] studied the use of *Ceratonia Siliqua L.* seed extract (CFE) as a green organic corrosion inhibitor for carbon steel in 1 M HCl. The GC-MS analysis technique showed that vanillin is the main constituent represented in the extract. The electrochemical test results showed that CEF shows a good anti-corrosion action with an inhibition efficiency (η%) of 95% at 100 mg/L at 298°C. Ghazi *et al.* [19] studied the effect of the Carob Pod Pulp (*Ceratonia siliqua L.*) corrosion inhibition on carbon steel C38 in 1 M HCl by using weight loss and electrochemical tests. Two raw extracts were prepared from Carob pod pulp (*Ceratonia siliqua L.*) aqueous and methanolic. The UHPLC/DAD analysis indicates that the garlic acids present in both extracts as a major compound. The inhibition results showed that the aqueous extract with garlic acid has a good

anti-corrosion efficiency with an inhibition efficiency (η%) of 91.32% at 3 g/L at 323°C. Fouda *et al.* [20] investigated the effect of the Carob pod (*Ceratonia silique)* extract on the corrosion of copper and brass in 1 M HNO_3. The electrochemical test results indicate that the extract can act as an effective corrosion inhibitor with an inhibition efficiency (η%) of 91% for copper and 98% for brass at 300 ppm at room temperature. Tafel curves show that the extract behaves as a mixed type with cathodic dominant. The adsorption behaviour of the extract on the copper and brass surface is physical and obeys Langmuir isotherm.

In summary, the efficiency of the seed extract was examined for low (mild) carbon steel with a carbon content of 0.157%, whereas the efficiency of the pod pulp extract was examined for medium carbon steel with a carbon content of approximately 0.37%. As a result, it is crucial to study the pod pulp extract for low (medium) carbon steel, as this will give researchers an understanding of its potential use as a green corrosion inhibitor for both low and medium carbon steel. Hence, this study attempts to examine the potential use of the pulp extracts as corrosion inhibitors of mild steel with carbon content (C: 0.08–0.12) in 1 M HCl at different concentrations of the extract. Accordingly, the inhibiting efficiency of the pulp versus that of the seed extract will be compared, especially as these different parts of the fruit may show differences in active substances. The development of such novel low-cost material from local green natural agro wastes has a promising impact on the economy and steel industry.

2. Experimental

2.1. Preparation of the material

Sheet metal of 0.1 cm thickness from Mild steel with a carbon content (0.08–0.12) wt.% was used to cut the test specimens. The detailed chemical composition of the steel is shown in Table 1 as provided from the supplier. Two sizes of square-shaped specimens were cut from sheet metal. Specimens with dimensions (6×6) cm^2 were used for potentiodynamic tests, and (3×3) cm^2 for the weight loss tests. The surface of the sample, except for a circle-shaped area in the middle of 1 cm^2, was covered with an adhesive that prevents the electrolyte from reaching the underlying metal. Before the corrosion test, the specimens were thoroughly washed with double distilled water, acetone, and ethanol. Then, the specimens were degreased ultrasonically with a bath of distilled water and ethanol for 5 minutes. Thereafter, the specimens were dried using an air dryer.

Table 1. Chemical composition of mild steel (wt.%).

Element	C	Si	Mn	S	P	Cr	Cu	As	Fe
wt.%	0.08–0.12	0.3	0.25–0.5	0.04	0.03	0.1	0.3	0.08	Bal.

2.2. Preparation of the inhibitor extract

Dried carob pods of *C. siliqua* were collected in June 2022 from carob trees at Jordan University of Science and Technology. The collected pods were washed with distilled water to remove dust and impurities. To produce pulp fine powder, the seeds were removed from the pods and the pulp was collected and ground using an electric mill. Then, 30 g of this powder was added to the organic solvent, which was composed of (135 ml of methanol, 135 ml of distilled water, and 30 ml of 1% of HCl), and mixed for 4 hours at room temperature using the magnetic stirrer. Then the mixture was filtered and centrifuged for 4 minutes at 4000 rpm. This procedure was repeated three times for efficient extraction. The rotary evaporator was used to dry all the centrifugal solutions. Finally, the produced solid mass was kept in the refrigerator at 4°C until used. Figure 1 presents the schematic steps of the used processes to produce *C. siliqua* pulp extracts as a green corrosion inhibitor of mild steel.

Figure 1. A schematic steps of the user processes to produce *C. siliqua* pulp extracts, a green corrosion inhibitor of mild steel.

2.3. Preparation of test solution

1 M HCl was prepared by diluting 91 ml of analytical grade 35.4% HCl with 909 ml of distilled water. This solution was used to create 4 types of solutions with different concentrations of *C. silique* pulp extracts (200, 400, 600, and 800 ppm) by adding a

predetermined amount of extracts directly to the solution. The 1 M HCl test solution was used as a blank for comparison and inhibitor efficiency calculation purposes.

2.4. Electrochemical cell setup

A flat cell provided by Gamry was used in this setup. The cut specimens with dimensions of (6×6 cm) and a thickness of 0.1 cm were used as working electrodes. The exposed area of the working electrode to the electrolyte was set as 1 cm^2. The counter electrode used was made of graphite, and the reference electrolyte was a saturated calomel electrode. 1 M HCl solution was used as an electrolyte in the control experiment. Then, other tests were conducted using 1 M HCl having different concentrations of extract as explained earlier.

2.5. Potentiodynamic polarization test

Before the polarization test, the samples were kept inside the electrolyte for 2.5 hours to reach steady state conditions. Then, the potentiodynamic polarization experiments started by polarizing the samples and shifting the potential from steady state condition, and measuring the resultant current. The start point was at 250 mV below the open circuit potential (OCP); then the applied potential was increased at a constant sweep rate of 1 mV/sec, and the test was terminated when the applied potential exceeded the OCP by 250 mV. A reference 600 potentiostat that was controlled with Gamry framework software version 7.9.1 was used to conduct these experiments. Furthermore, Gamry Echem Analyst software was used to analyze the polarization curves and extract the corrosion parameters including the corrosion current density (i_{corr}), free corrosion potential (E_{corr}), and Tafel anodic and cathodic slopes (β_a, β_c) through the Tafel extrapolation method by using an interval of 100 mV around E_{corr} value.

2.6. Weight loss tests

The researchers have used the weight loss method in measuring the corrosion rate extensively because of its simplicity and availability [21]. Firstly, the specimens were cleaned, dried, and weighted using Ariston Digital balance. Then, they were fully immersed in 100 ml of the HCl solution with the presence and absence of different concentrations of *C. siliqua* pulp extracts at room temperature. After 2 hours of immersion time, the specimens were removed from the corrosive solution, rinsed with acetone, ethanol, and distilled water, dried with an air dryer, and reweighed. To examine the effect of time, the experiments were repeated at immersion times of 4, 6, 24, and 48 hours, where three replicates of each experiment were conducted. The weight's loss are then used to calculate the corrosion rate.

The following equation was used to calculate the weight loss at a given time:

$$\Delta w = w_0 - w_i \tag{1}$$

where Δw – specimen's weight loss, w_0 – weight loss of the specimen without inhibitors, w_i – weight loss of the specimen with inhibitors.

From the weight loss data, the corrosion rate, inhibition efficiency, and surface coverage were calculated using equations 2, 3, and 4 respectively [22, 23].

$$CR(\text{mpy}) = \frac{534 \cdot \Delta w}{\rho \cdot A \cdot t} \tag{2}$$

where *CR* – corrosion rate (mpy), Δw – average weight loss (mg), ρ – density of the mild steel (7.78 g/cm^3), *A* – area of the mild steel sample (cm^2), and *t* – the immersion time.

Thereafter, for each test condition (inhibitor concentration and time), 3 replicates were conducted, and then the average corrosion rate values were computed from these parallel experiments. This is because corrosion is a random process and the weight loss of individual samples may vary due to random fluctuations in the test conditions, and the microstructure of the samples. By using the average of multiple replicate samples, the variability in the results can be reduced and a more accurate representation of the corrosion rate can be obtained. This helps to improve the reliability of the weight loss test results and provides a more robust estimate of the effectiveness of the inhibitor.

$$\%I.E. = \left(\frac{CR_0 - CR}{CR_0} \right) \cdot 100\% \tag{3}$$

$$\theta = \frac{CR_0 - CR}{CR} \tag{4}$$

where *%I.E.* – percentage of inhibition efficiency, θ – degree of the surface coverage, CR_0 – corrosion rate of the substrates without inhibitor (mpy), and *CR* – corrosion rate of the substrates with inhibitor (mpy).

3. Result and Discussion

3.1. Potentiodynamic polarization test

The polarization curves (plot of (*E*) versus (log*i*) in the Tafel region obtained for the mild steel specimens in 1 M HCl solution at room temperature with the presence and absence of different concentrations of *C. siliqua* pulp extracts are shown in Figure 2.

The electrochemical parameters such as corrosion potential (E_{corr}), corrosion current density (i_{corr}), polarization resistance(R_p), and the cathodic and anodic Tafel slopes (β_c, β_a respectively) [24] are obtained from the Tafel extrapolation method and listed in Table 2. The percentage of inhibition efficiency (η%) that is given in Table 2 was calculated using the following equation [25].

$$\eta(\%) = \left(\frac{i_{corr}^0 - i_{corr}}{i_{corr}^0} \right) \cdot 100\% \tag{5}$$

where i^0_{corr} – corrosion current density with the absence of *C. siliqua* pulp extract in 1 M HCl (μA/cm^2), i_{corr} – corrosion current density with the presence of *C. siliqua* pulp extract in 1 M HCl (μA/cm^2).

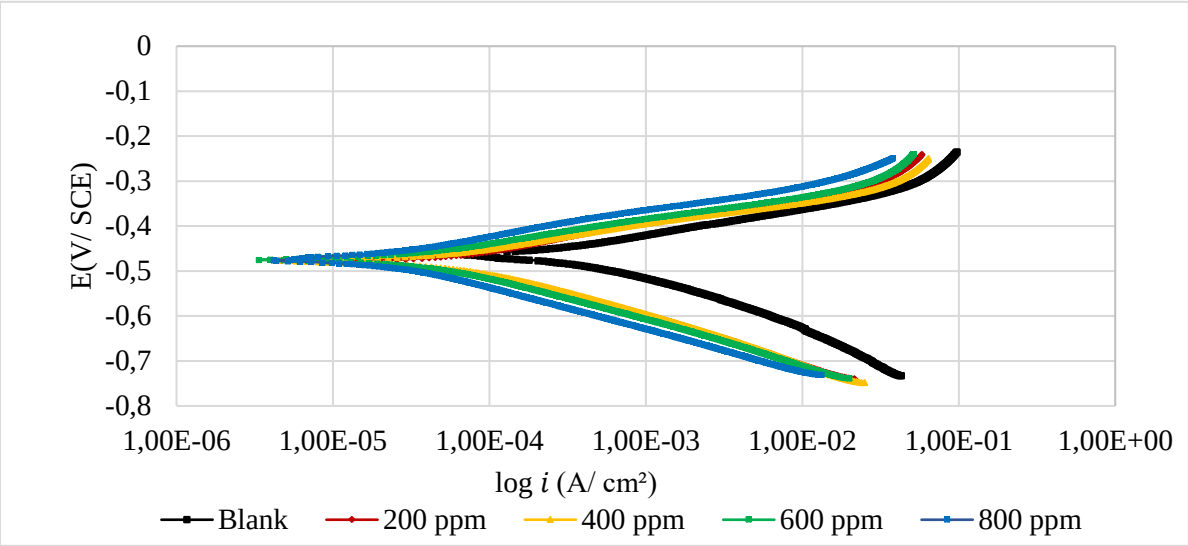

Figure 2. Tafel plots of mild steel in 1 M HCl in the absence and presence of different concentrations of *C. siliqua* pulp extract at room temperature.

Polarization resistance (R_p) can be calculated using the Stern-Geary equation [26]:

$$R_p = \frac{\beta_c \cdot \beta_a}{2.303 \cdot i_{corr} (\beta_c + \beta_a)} \quad (6)$$

where β_c – Tafel cathodic slopes (V/decade), β_a – Tafel anodic slopes (V/decade), i_{corr} – corrosion current density with the presence of *C. siliqua* pulp extract in 1 M HCl (μA/cm^2).

Table 2. The electrochemical parameters (derived from Figure 2) for the mild steel in 1 M HCl in the absence and presence of different concentrations of *C. siliqua* pulp extract at room temperature. Values are the mean of the three repeats and (±) corresponds to standard deviations.

C_{inh} (ppm)	$\beta_a \cdot 10^{-3}$ (V/decade)	$-\beta_c \cdot 10^{-3}$ (V/decade)	i_{corr} (μA/cm^2)	E_{corr} (mV)	R_p (Ω·cm^2)	CR (mpy)	η (%)
Blank	70±12	96±7	264±43	–464±12	0.5±0.3	121±20	–
200	74±6	94±9	59±8	–481±9	3±1	27±4	77.56
400	64±1	86±1	48±5	–477±3	2±0	22±2	81.64
600	63±3	89±1	33±1	–474±3	3±1	15±0	87.49
800	69±4	91±12	20±4	–474±5	8±6	9±2	92.35

It is clear from Figure 2 and Table 2 that in the presence of *C. siliqua* pulp extract, the current density decreased, which may arise from covering the inhibitor molecules on the

mild steel surface. These results suggested that the addition of inhibitors reduces the anodic dissolution and delays the hydrogen evaluation reactions. Furthermore, a slight shift was observed in the values of cathodic and anodic Tafel slopes with the presence of *C. siliqua* pulp extract, which indicates that the inhibitor act as an efficient corrosion inhibitor of the mild steel in 1 M HCl. This is because the inhibitor molecules are getting adsorbed on the mild steel surface, resulting in blocking the active sites without changing the corrosion reaction mechanisms. Thus, both anodic dissolution and hydrogen evaluation reactions are suppressed. In addition, the displacements in the E_{corr} value were less than 85 mV with respect to the blank mild steel sample this result indicates that the *C. siliqua* pulp extract act as a mixed-type inhibitor, and the cathodic impact is predominant [27]. The increase in R_p values with the addition of *C. siliqua* pulp extract in 1 M HCl suggests effective inhibition performance in the presence of *C. siliqua* pulp extract molecules that act to enhance the polarization process at the metallic acid interface by adsorption of the inhibitor on the metal surface and blocking the active sites [28].

3.2. Weight loss test

3.2.1. Effect of concentrations

The spontaneous dissolution of the mild steel in 1 M HCl in the presence of *C. siliqua* pulp extract as a corrosion inhibitor was studied by weight loss test at room temperature after 2 hours of immersion time. The corrosion parameters such as corrosion rate (*CR*), Inhibition efficiency (%*I.E.*), and the degree of the surface coverage (θ) are calculated by equations 2, 3, and 4 respectively, listed in Table 3, and presented graphically in Figures 3 and 4.

Table 3. Corrosion parameters for the mild steel in 1 M HCl solution with and without different concentrations of *C. siliqua* pulp extract from the weight loss test after 2 hours of immersing time at room temperature. Values are the mean of the three repeats and (±) corresponds to standard deviations.

Concentration (ppm)	**Weight loss (mg)**	**Corrosion rate (mpy)**	**Inhibition Efficiency (%*I.E.*)**	**Degree of the surface coverage (θ)**
0	46±19	$1.7\times10^3\pm0.7\times10^3$		
200	37±4	$1.4\times10^3\pm0.2\times10^3$	19%	0.19
400	25±3	$0.9\times10^3\pm0.1\times10^3$	46%	0.46
600	21±2	$0.8\times10^3\pm0.1\times10^3$	52%	0.55
800	18±1	$0.7\times10^3\pm0.1\times10^3$	61%	0.61

It is evident from Table 3, Figures 3, and 4 that the mild steel corrosion rate decreased with the increase in the concentration of *C. siliqua* pulp extract. Accordingly, the values of the inhibition efficiency of *C. siliqua* pulp extract increased with increasing concentration which reached 59.65% at 800 ppm. This inhibition behaviour can be explained by the

adsorption of the *C. siliqua* pulp extract molecules at high concentrations on the mild steel surface. This leads to wider surface coverage and the formation of a productive film. Furthermore, the metal substrate's surface coverage (θ) gradually increases whenever the inhibitor concentration increases. This is because the inhibitor acts as an adsorbent, the metal surface acts as an adsorbate, and it forms a barrier layer over the mild steel surface. Thus, blocking the reaction sites, and protecting the surface from corrosion attacks and dissolution in the acidic media. Hence, the inhibition efficiency increased and the corrosion rate decreased as the adsorbed molecules covering the mild steel surface increased [4, 29].

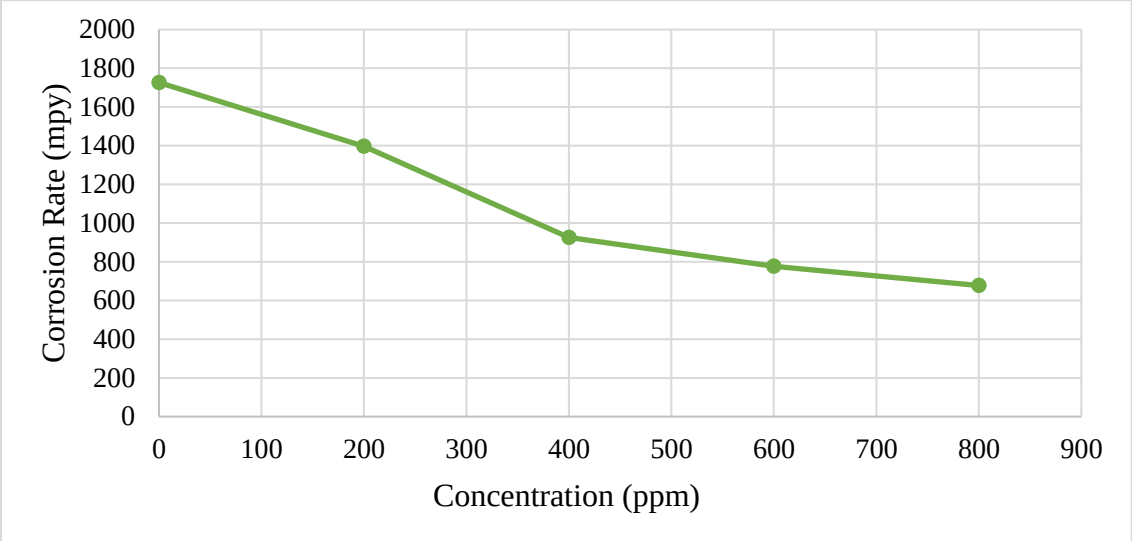

Figure 3. Change of the mild steel corrosion rate as calculated from the weight loss test with different concentrations of *C. siliqua* pulp extract in 1 M HCl at room temperature.

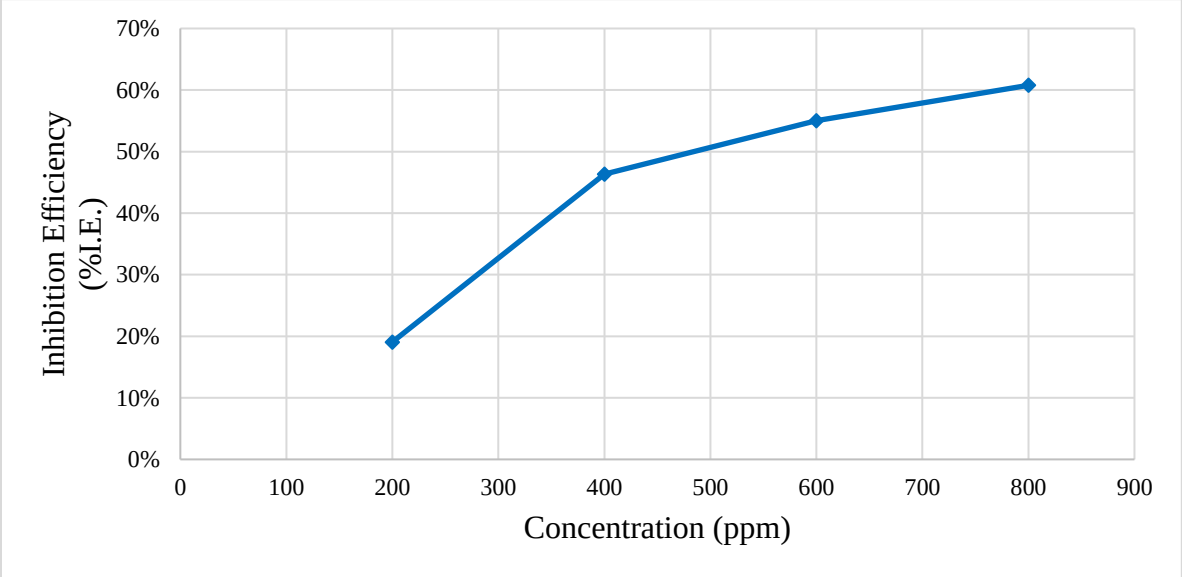

Figure 4. Change of the inhibition efficiency Inhibition efficiency (%*I.E.*) of the mild steel in various concentrations of *C. siliqua* pulp extract as calculated from the weight loss test in 1 M HCl at room temperature.

3.2.2. Effect of immersion time

Immersion time is another important parameter in assessing the inhibitor's behavior, inhibition efficiency, and corrosion rate for a prolonged immersion period. The inhibition efficiency (%*I.E.*) values and the corrosion rate that was obtained from the weight loss test at different concentrations of *C. siliqua* pulp extract in 1 M HCl and at different immersion times 4, 6, 24 and 48 hours at room temperature are listed in Table 4 and 5 and graphically presented in Figure 5.

Table 4. Corrosion rate (mpy) values for the mild steel in 1 M HCl solution in the absence and presence of different concentrations of *C. siliqua* pulp extract from the weight loss measurements after different immersion times at room temperature. Values are the mean of the three replicates and (±) corresponds to standard deviations.

Time (h)	Corrosion Rate (mpy) $\times 10^3$				
	Concentration (ppm)				
	Blank	200 (ppm)	400 (ppm)	600 (ppm)	800 (ppm)
2	1.7±0.7	1.4±0.2	0.9±0.1	0.8±0.1	0.7±0.1
4	1.7±0.3	1.1±0.1	0.7±0.1	0.7±0.1	0.5±0.0
6	1.7±0.4	1.0±0.1	0.7±0.1	0.6±0.1	0.4±0.0
24	1.9±0.1	1.1±0.0	0.7±0.1	0.5±0.0	0.4±0.0
48	2.1±0.2	1.0±0.0	0.7±0.1	0.4±0.1	0.3±0.0

Table 5. The corrosion inhibition efficiency (%*I.E.*) values for the mild steel in 1 M HCl solution in the absence and presence of different concentrations of *C. siliqua* pulp extract from the weight loss measurements after different immersion times at room temperature.

Time (h)	The Inhibition Efficiency (%*I.E.*)			
	Concentration (ppm)			
	200 (ppm)	400 (ppm)	600 (ppm)	800 (ppm)
2	19%	46%	55%	61%
4	33%	58%	62%	70%
6	40%	62%	67%	75%
24	45%	66%	75%	81%
48	50%	69%	79%	86%

It is clear from Tables 4 and 5 and Figure 5 that for all examined concentration of *C. siliqua* pulp extract, the maximum inhibition efficiency and the minimum corrosion rate was

recorded after 48 hours of immersion time. The inhibition efficiency (%*I.E.*) increases and the corrosion rate (C_R) decreases with the immersion time. This is because at relatively low concentrations considerable time is required for sufficient adsorption of the inhibitor molecules on the metal surfaces to take place [30]. Furthermore, this indicates the stability and persistence of *C. siliqua* pulp extract films on the mild steel surface in acidic solutions which could remain for quite a long time [31]. Moreover, the inhibition efficiency (%*I.E.*) increased with time due to the formation of inhibitor complexes over the metal surface and the construction of strong bonds with the substrate atoms. Apparently, as time increased, these complexes' production rates increased, resulting in higher efficiency and more restrictions on the corrosive electrolyte to reach the metal surfaces [32]. This leads to a broader surface cover. Thus, blocking the reaction sites, and protecting the metal surfaces from corrosion attack and dissolution in acidic media [4]. These results are consistent with the results reported in the literature. It should be mentioned that the inhibition efficiency obtained from the weight loss test is lower than the corresponding values attained from the potentiodynamic polarization test at the same concentration level. This difference can be explained by the weight loss test gives an average corrosion rate, whereas the potentiodynamic polarization test gives an instantaneous corrosion rate. The difference in time required to form an adsorbed layer of inhibitors on the metal surface is in charge of these differences [33].

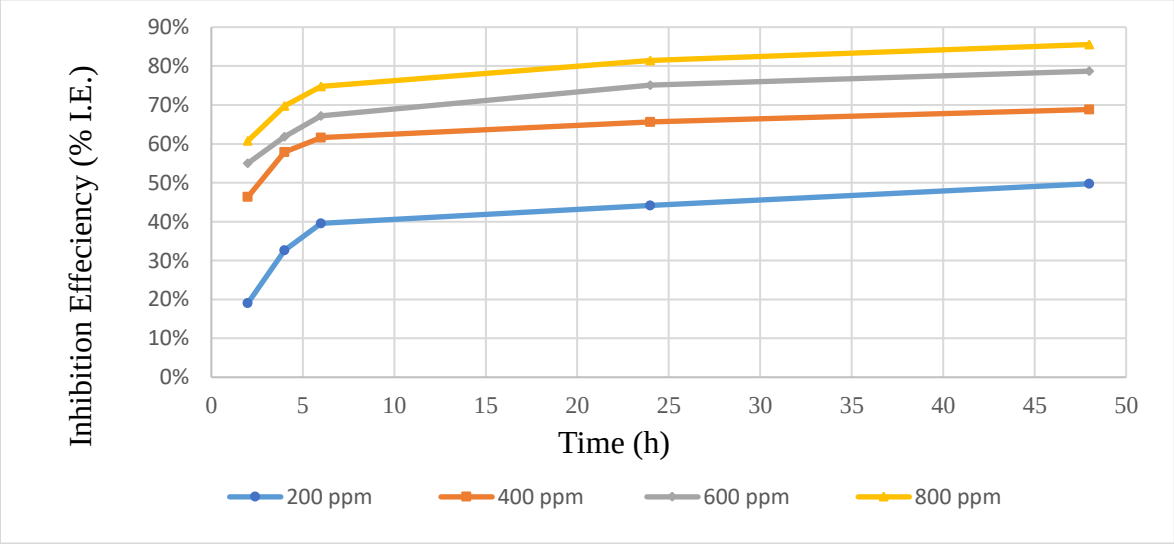

Figure 5. Variation of corrosion inhibition efficiency (%*I.E.*) values for the mild steel in 1 M HCl solution in the absence and presence of different concentrations of *C. siliqua* pulp extract from the weight loss measurements after different immersion times at room temperature.

3.3. Adsorption isotherm

Adsorption isotherms provide information about the behavior of adsorption and the nature of the interactions between the inhibitor molecules and the surface of the metal by fitting a

relationship between the surface coverage and the inhibitor concentrations. However, many isotherms' models are mentioned in the literature, but Langmuir, Temkin, and Frumkin are the most widely used. The selection of the isotherm model should be based on a thorough analysis of the experimental data. One commonly used technique is to fit multiple isometric models to the data and compare the goodness of fit using statistical measures, such as the correlation coefficient (R^2). Ultimately, the best isothermal model for a given system provides the best fit to the experimental data, accurately describes the underlying adsorption mechanism and is practical to implement. However, these models are used in the investigation of the adsorption mechanism of the corrosion inhibitors, which can be calculated by the following equations [25]:

Langmuir: $$\frac{c}{\theta} = \frac{1}{k_{ads}} + c \quad (7)$$

Temkin: $$\exp(f \cdot \theta) = k_{ads} \cdot c \quad (8)$$

Frumkin: $$\frac{\theta}{1-\theta}\exp(-2f) = k_{ads} \cdot c \quad (9)$$

where c – inhibitor concentrations 50, 200, 500, and 800 ppm, θ – the degree of the surface coverage, which is evaluated according to Equation 4, f – corrosion inhibitor interaction parameter, k_{ads} – the adsorption equilibrium constant (which represents the degree of adsorption, *i.e.*, the higher value of k_{ads} indicates that the inhibitor is strongly adsorbed on the surface of the metal).

Figures 6, 7, and 8 show the plots obtained from Equations 7, 8, and 9. The correlation coefficients R^2 values, and slope of the fitting line for each model were used to determine the most suitable model and are presented in Table 6.

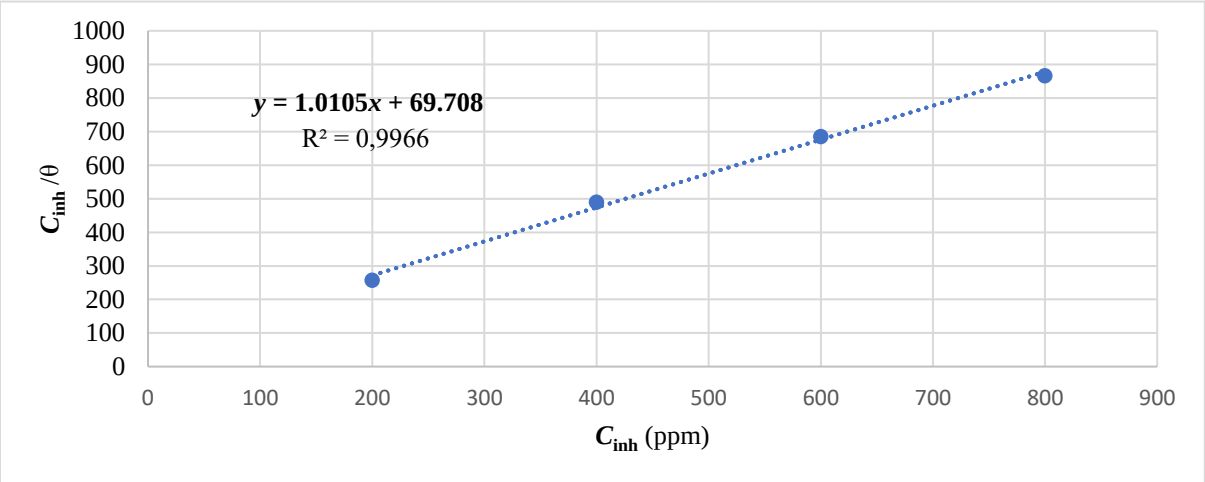

Figure 6. Plot for the Langmuir isotherm for adsorption of *C. siliqua* pulp extract on the mild steel surface in 1 M HCl at room temperature.

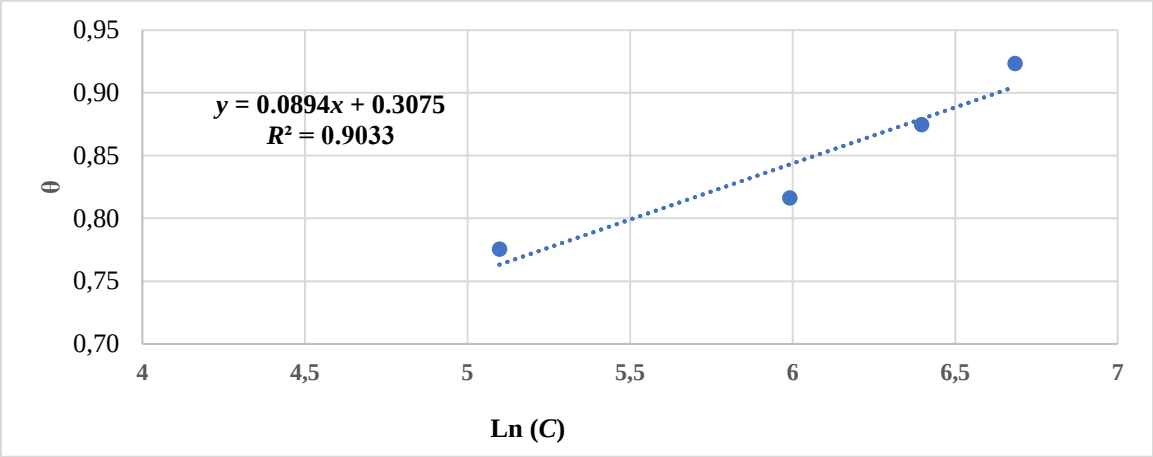

Figure 7. Plot for the Temkin isotherm for adsorption of *C. siliqua* pulp extract on the mild steel surface in 1 M HCl at room temperature.

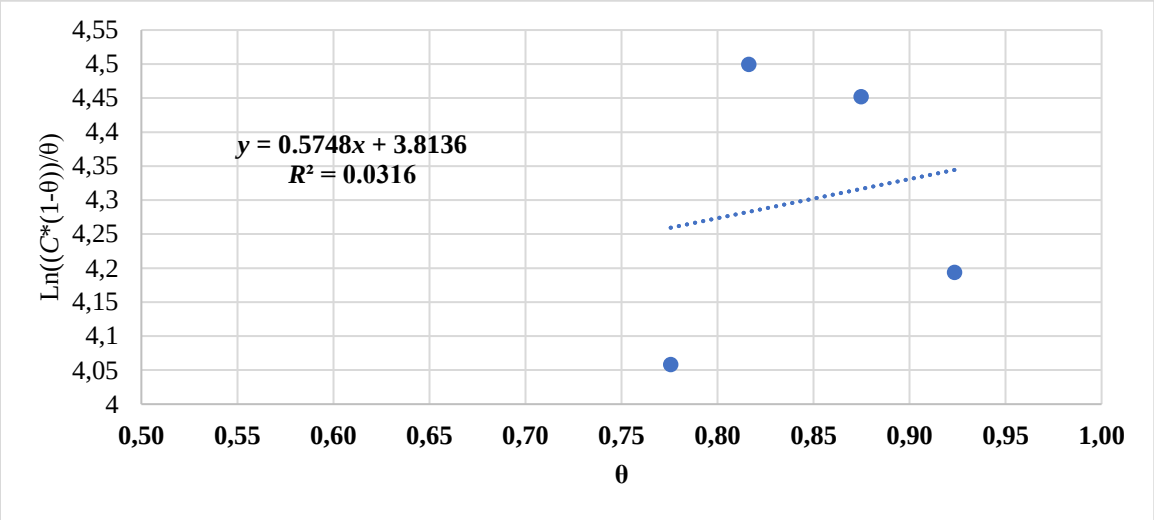

Figure 8. Plot for the Frumkin isotherm for adsorption of *C. siliqua* pulp extract on the mild steel surface in 1 M HCl at room temperature.

Table 6. R^2 values and the slopes for Langmuir, Temkin, and Frumkin isotherms for *C. silique* pulp extract.

***C. silique* pulp extract**	**Langmuir**	**Temkin**	**Frumkin**
R^2	0.997	0.903	0.032
Slope	1.011	0.089	0.575

From the plots' observations, the graphic relation between the C/θ *vs.* C is presented in Figure 6. Through the observations, the Langmuir adsorptions calculated by Equation 7 were found to be consistent with the data of the potentiodynamic polarization test. Straight lines with almost unity slopes (1.015) and a correlation coefficient R^2 is 0.997 are obtained as represented in Table 6 which are better than the slope and correlation coefficients for Temkin and Frumkin isotherms in Figure 7 and Figure 8. These results indicate that adsorption of

the *C. siliqua* pulp extract organic matter obeys Langmuir isotherm. Langmuir isotherms assume that the adsorption of each molecule on the surface is independent of the other molecules and that the adsorbed surface is homogeneous and has a finite number of adsorption sites [34].

3.4. Determination of adsorption mechanisms

The standard adsorption-free energy ΔG_{ads}^0 was used to investigate the mechanism of the adsorption of the inhibitors. However, the values ΔG_{ads}^0 were calculated according to the following Equation 10 to determine the adsorption mechanism:

$$\Delta G_{ads}^0 = -RT \ln\left(55.5 k_{ads}\right) \tag{10}$$

where R – gas constant 8.314 J/mol, T – absolute temperature, 298 K, 55.5 is the molar concentration of water (factor 55.5 $\text{mol}\cdot\text{L}^{-1}$ was substituted with 1000 $\text{g}\cdot\text{L}^{-1}$ to meet the units of K_{ads} [4]), k_{ads} is the adsorption equilibrium constant ($\text{L}\cdot\text{g}^{-1}$).

Generally, the negative values of the ΔG_{ads}^0 indicate that the adsorption process of the extracted inhibitor is spontaneous and stable. Moreover, as reported in the literature, the absolute value of $\Delta G_{ads}^0 \leq 20$ kJ/mol is regarded as a physisorption mechanism related to an electrostatic interaction between the positive charge molecules of the extracted inhibitor and the negative charge of the metal surface. On the other hand, the absolute values of $\Delta G_{ads}^0 \geq 40$ kJ/mol was regarded as a chemisorption mechanism, which involved forming a chemical bonding between the extracted inhibitor molecules and the metal surface through electron transfer or sharing Moreover, the values of ΔG_{ads}^0 between these ranges are usually attributed to a mixed mechanism, which is sometimes called physiochemiosorption [35, 36]. The ΔG_{ads}^0 values in this work was (–23.958 kJ/mol) for *C. siliqua* pulp extract, manifesting the adsorption of *C. siliqua* pulp extract on the surface of mild steel is related to physical adsorption.

4. Conclusions

The inhibition performance, as well as the related mechanism of *C. siliqua* pulp extract for mild steel protection in 1 M HCl, have been studied, and the following are major conclusions:

1. *C. siliqua* pulp extract is an effective corrosion inhibitor for mild steel with carbon content (C: 0.08–0.12) in 1 M HCl. The maximum inhibition efficiency obtained was 92.35% at a concentration of 800 ppm at room temperature. Therefore, the efficiency of the pulp extracts is comparable to that obtained by other researchers from seed extracts for steel with a carbon content of 0.157% which was approximately 95% at 100 mg/L [18].
2. Potentiodynamic polarization tests suggest that *C. siliqua* pulp extract acts as a mixed-type inhibitor, and the cathodic impact is predominated.

3. The weight loss test results demonstrate that *C. siliqua* pulp extract efficiency increase with concentration and immersion time.
4. The adsorption mechanism for *C. siliqua* pulp extract on the mild steel surface follows the Langmuir adsorption isotherm.
5. The ΔG^0_{ads} values indicate that the *C. siliqua* pulp extract adsorption process is spontaneous and stable, and it is adsorbed on the mild steel surface by physical adsorption.

Funding

This work was supported by a grant from the Deanship of Scientific Research at Jordan University of Science and Technology (JUST) with grant no.166/2019.

References

1. M. Rbaa, M. Fardioui, C. Verma, A. Abousalem, M. Galai, E.E. Ebenso, T. Guedira, B. Lakhrissi, I. Warad and A. Zarrouk, 8-Hydroxyquinoline based chitosan derived carbohydrate polymer as biodegradable and sustainable acid corrosion inhibitor for mild steel: Experimental and computational analyses, *Int. J. Biol. Macromol*., 2020, **155**, 645–655. doi: 10.1016/j.ijbiomac.2020.03.200
2. H. Zhang and Y. Chen, Experimental and theoretical studies of benzaldehyde thiosemicarbazone derivatives as corrosion inhibitors for mild steel in acid media, *J. Mol. Struct*., 2019, **1177**, 90–100. doi: 10.1016/j.molstruc.2018.09.048
3. M.K. Pal and M. Lavanya, Corrosion of mild steel: a microbiological point of view, *Can. Metall. Q*., 2022, **61**, no. 3, 292–308. doi: 10.1080/00084433.2022.2046907
4. M. Mobin, M. Basik and J. Aslam, Pineapple stem extract (bromelain) as an environmentally friendly novel corrosion inhibitor for low carbon steel in 1 M HCl, *Measurement*, 2019, **134**, 595–605. doi: 10.1016/j.measurement.2018.11.003
5. A. Ghazoui, N. Benchat, F. El-Hajjaji, M. Taleb, Z. Rais, R. Saddik, A. Elaatiaoui and B. Hammouti, The study of the effect of ethyl (6-methyl-3-oxopyridazin-2-yl) acetate on mild steel corrosion in 1 M HCl, *J. Alloys Compd*., 2017, **693**, 510–517. doi: 10.1016/j.jallcom.2016.09.191
6. H.J. Habeeb, H.M. Luaibi, R.M. Dakhil, A.A. Kadhum, A.A. Al-Amiery and T.S. Gaaz, Development of new corrosion inhibitor tested on mild steel supported by electrochemical study, *Results Phys*., 2018, **8**, 1260–1267. doi: 10.1016/j.rinp.2018.02.015
7. Z. Sanaei, M. Ramezanzadeh, G. Bahlakeh and B. Ramezanzadeh, Use of *Rosa canina* fruit extract as a green corrosion inhibitor for mild steel in 1 M HCl solution: A complementary experimental, molecular dynamics and Quantum Mechanics Investigation, *J. Ind. Eng. Chem*., 2019, **69**,18–31. doi: 10.1016/j.jiec.2018.09.013
8. S.A. Umoren, M.M. Solomon, I.B. Obot and R.K. Suleiman, A critical review on the recent studies on plant biomaterials as corrosion inhibitors for industrial metals, *J. Ind. Eng. Chem*., 2019, **76**, 91–115. doi: 10.1016/j.jiec.2019.03.057

9. B. Brycki, I. Kowalczyk, A. Szulc, O. Kaczerewska and M. Pakiet, Organic corrosion inhibitors, *Corrosion Inhibitors, Principles, and Recent Application*, Cambridge, MA: Elsevier, 2018. doi: 10.5772/intechopen.72943
10. M. Jokar, T. Farahani and B. Ramezanzadeh, Electrochemical and surface characterizations of Morus alba pendula leaves extract (maple) as a green corrosion inhibitor for steel in 1 M HCl, *J. Taiwan Inst. Chem. Eng*., 2016, **63**, 436–452. doi: 10.1016/j.jtice.2016.02.027
11. C.B. Verma, A. Singh, G. Pallikonda, M. Chakravarty, M.A. Quraishi, I. Bahadur and E.E. Ebenso, Aryl sulfonamidomethylphosphonates as a new class of green corrosion inhibitors for mild steel in 1 M HCl: Electrochemical, surface and quantum chemical investigation, *J. Mol. Liq*., 2016, **209**, 306–319. doi: 10.1016/j.molliq.2015.06.013
12. G. Bahlakeh, A. Dehghani, B. Ramezanzadeh and M. Ramezanzadeh, Highly effective mild steel corrosion inhibition in 1 M HCl solution by novel green aqueous *Mustard* seed extract: Experimental, electronic-scale DFT and atomic-scale MC/MD explorations, *J. Mol. Liq*., 2019, **293**, 111559. doi: 10.1016/j.molliq.2019.111559
13. N. Hossain, M.A. Chowdhury and M. Kchaou, An overview of green corrosion inhibitors for sustainable and Environment-Friendly Industrial Development, *J. Adhes. Sci. Technol*., 2021, **35**, no. 7, 673–690 doi: 10.1080/01694243.2020.1816793
14. N. Benmansour, Study of the biological activities of the seeds of the plant ceratonia siliqua L. recovered in the bejaia region, *J. Med. Technol*., 2020, **4**, no. 1, 520–521.
15. L.M. Dos Santos, L.T. Tulio, L.F. Campos, M.R. Dorneles and C.C. Hecke Krüger, Res puesta glucémica de algarrobo (*Ceratonia siliqua L*) en sujetos sanos y con el índice de hidrólisis in vitro, *Nutr. Hosp*., 2015, **31**, no. 1, 482–487. doi: 10.3305/nh.2015.31.1.8011
16. B.J. Zhu, M.Z. Zayed, H.X. Zhu, J. Zhao and S.P. Li, Functional polysaccharides of Carob Fruit: A Review, *Chin. Med*., 2019, **14**, no. 40. doi: 10.1186/s13020-019-0261-x
17. I.J. Stavrou, A. Christou and C.P. Kapnissi-Christodoulou, Polyphenols in carobs: A review on their composition, antioxidant capacity and cytotoxic effects, and Health Impact, *Food Chem*., 2018, **269**, 355–374. doi: 10.1016/J.FOODCHEM.2018.06.152
18. S. Abbout, D. Chebabe, M. Zouarhi, M. Rehioui, Z. Lakbaibi and N. Hajjaji, *Ceratonia Siliqua L* seeds extract as eco-friendly corrosion inhibitor for carbon steel in 1 M HCl: Characterization, electrochemical, surface analysis, and theoretical studies, *J. Mol. Struct*., 2021, **1240**, 130611. doi: 10.1016/j.molstruc.2021.130611
19. I. Ghazi, M. Zefzoufi, M. Siniti, R. Fdil and H. Elattari, Corrosion Inhibition of Carob Pod Pulp (*Ceratonia siliqua L.*) on Carbon Steel Surface C38 in Hydrochloric Acid, *J. Bio- Tribo- Corros*., 2022, **8**, no. 1, 1–23. doi: 10.1007/s40735-022-00630-y
20. A.S. Fouda, K. Shalabi and A.A. Idress, Ceratonia siliqua extract as a green corrosion inhibitor for copper and brass in nitric acid solutions, *Green Chem. Lett. Rev*., 2015, **8**, no. 3–4, 17–29. doi: 10.1080/17518253.2015.1073797

21. E.B. Agbaffa, E.O. Akintemi, E.A. Uduak and O.E. Oyeneyin, Corrosion inhibition potential of the methanolic crude extract of Mimosa pudica leaves for mild steel in 1 M hydrochloric acid solution by weight loss method, *J. Sci. Lett*., 2021, **15**, no. 1, 23–42. doi: 10.24191/sl.v15i1.11791
22. M.H. Sliem, M. Afifi, A.B. Radwan, E.M. Fayyad, M.F. Shibl, F.E.T. Heakal and A.M. Abdullah, AEO7 surfactant as an eco-friendly corrosion inhibitor for carbon steel in HCl Solution, *Sci. Rep*., 2019, **9**, no. 1, 1–16. doi: 10.1038/s41598-018-37254-7
23. P. Muthukrishnan, P. Prakash, B. Jeyaprabha and K. Shankar, Stigmasterol extracted from *Ficus hispida* leaves as a green inhibitor for the mild steel corrosion in 1 M HCl solution, *Arabian J. Chem*., 2019, **12**, no. 8, 3345–3356. doi: 10.1016/j.arabjc.2015.09.005
24. G. Fekkar, F. Yousfi, H. Elmsellem, M. Aiboudi, M. Ramdani, A. Rahman, B. Hammouti and L. Bouyazza, Eco-friendly *chamaerops humilis L.* Fruit extract corrosion inhibitor for mild steel in 1 M HCl, *Int. J. Corros. Scale Inhib*., 2020, **9**, no. 2, 446–459. doi: 10.17675/2305-6894-2020-9-2-4
25. W. Zhang, H.J. Li, M. Wang, L.J. Wang, A.H. Zhang and Y.C. Wu, Highly effective inhibition of mild steel corrosion in HCl solution by using pyrido[1,2-a]benzimidazoles, *New J. Chem*., 2019, **43**, no. 1, 413–426. doi: 10.1039/C8NJ04028A
26. A. Singh, I. Ahamad, V. Singh and M. Quraishi, Inhibition effect of environmentally benign Karanj (*pongamia pinnata*) seed extract on corrosion of mild steel in hydrochloric acid solution, *J. Solid State Electrochem*., 2011, **15**, no. 6, 1087–1097. doi: 10.1007/s10008-010-1172-z
27. N. Yilmaz, A. Fitoz, ÿmit Ergun and K. Emregül, A combined electrochemical and theoretical study into the effect of 2-((thiazole-2-ylimino)methyl) phenol as a corrosion inhibitor for mild steel in a highly acidic environment, *Corros. Sci*., 2016, **111**, 110–120. doi: 10.1016/j.corsci.2016.05.002
28. G. Karthik and M. Sundaravadivelu, Studies on the inhibition of mild steel corrosion in hydrochloric acid solution by Atenolol Drug, *Egypt. J. Pet*., 2016, **25**, no. 2, 183–191. doi: 10.1016/J.EJPE.2015.04.003
29. J. Bhawsar, P.K. Jain and P. Jain, Experimental and computational studies of *Nicotiana tabacum* leaves extract as green corrosion inhibitor for mild steel in acidic medium, *Alexandria Eng. J*., 2015, **54**, no. 3, 769–775. doi: 10.1016/j.aej.2015.03.022
30. O.A. Akinbulumo, O.J. Odejobi and E.L. Odekanle, Thermodynamics and adsorption study of the corrosion inhibition of mild steel by *Euphorbia heterophylla L.* extract in 1.5 M HCl, *Results Mater*., 2020, **5**, 100074. doi: 10.1016/j.rinma.2020.100074
31. R. Karthikaiselvi, S. Subhashini and R. Rajalakshmi, Poly (vinyl alcohol – aniline) water-soluble composite as corrosion inhibitor for mild steel in 1 M HCL, *Arabian J. Chem*., 2012, **5**, no. 4, 517–522. doi: 10.1016/j.arabjc.2010.09.020
32. M.T. Majd, S. Asaldoust, G. Bahlakeh, B. Ramezanzadeh and M. Ramezanzadeh, Green method of carbon steel effective corrosion mitigation in 1 M HCl medium protected by *Primula vulgaris* flower aqueous extract via experimental, atomic-level MC/MD

Simulation and Electronic-level DFT Theoretical Elucidation, *J. Mol. Liq*., 2019, **284**, 658–674. doi: 10.1016/j.molliq.2019.04.037

33. M.P. Chakravarthy, C.B.P. Kumar and K.N. Mohana, Adsorption and corrosion inhibition characteristics of some nicotinamide derivatives on mild steel in hydrochloric acid solution, *Int. J. Ind. Chem*., 2014, **5**, no. 2, 1–13. doi: 10.1007/s40090-014-0019-3
34. H. Hassannejad and A. Nouri, Sunflower seed hull extract as a novel green corrosion inhibitor for mild steel in HCl Solution, *J. Mol. Liq*., 2018, **254**, 377–382. doi: 10.1016/j.molliq.2018.01.142
35. E. Ituen, O. Akaranta and A. James, Evaluation of Performance of Corrosion Inhibitors Using Adsorption Isotherm Models: An Overview, *Int. J. Chem. Sci*., 2017, **18**, no. 1, 1–34.
36. Q. Wang, B. Tan, H. Bao, Y. Xie, Y. Mou, P. Li, D. Chen, Y. Shi, X. Li and W. Yang, Evaluation of *ficus tikoua* leaves extract as an eco-friendly corrosion inhibitor for carbon steel in HCl Media, *Bioelectrochemistry*, 2019, **128**, 49–55. doi: 10.1016/j.bioelechem.2019.03.001

♦ ♦ ♦